JCI insight

RESEARCH ARTICLE

Disrupting the IL-36 and IL-23/IL-17 loop underlies the efficacy of calcipotriol and corticosteroid therapy for psoriasis

Beatriz Germán,[1,2,3,4] Ruicheng Wei,[1,2,3,4] Pierre Hener,[1,2,3,4] Christina Martins,[5] Tao Ye,[1,2,3,4] Cornelia Gottwick,[6] Jianying Yang,[6] Julien Seneschal,[5] Katia Boniface,[5] and Mei Li[1,2,3,4]

[1]Institut de Génétique et de Biologie Moléculaire et Cellulaire, Illkirch, France. [2]Centre National de la Recherche Scientifique, UMR7104, Illkirch, France. [3]Institut National de la Santé et de la Recherche Médicale, U1258, Illkirch, France. [4]Université de Strasbourg, Illkirch, France. [5]INSERM U1035, BMGIC, Equipe Immunodermatologie ATIP-AVENIR, Hôpital Saint-André Service de Dermatologie, Université de Bordeaux, France. [6]BIOSS Centre for Biological Signalling Studies, Department of Molecular Immunology, Institute of Biology III, Faculty of Biology, University of Freiburg, Freiburg, Germany

Psoriasis is one of the most common skin inflammatory diseases worldwide. The vitamin D3 analog calcipotriol has been used alone or in combination with corticosteroids in treating plaque psoriasis, but how it suppresses psoriatic inflammation has not been fully understood. Using an experimental mouse psoriasis model, we show that topical calcipotriol inhibited the pivotal IL-23/IL-17 axis and neutrophil infiltration in psoriatic skin, and interestingly, such effects were mediated through the vitamin D receptor (VDR) in keratinocytes (KCs). We further reveal that IL-36α and IL-36γ, which have recently emerged as key players in psoriasis pathogenesis, were effectively repressed by calcipotriol via direct VDR signaling in mouse KCs. Accordingly, calcipotriol treatment suppressed IL-36α/γ expression in lesional skin from patients with plaque psoriasis, which was accompanied by a reduced IL-23/IL-17 expression. In contrast, dexamethasone indirectly reduced IL-36α/γ expression in mouse psoriatic skin through immune cells. Furthermore, we demonstrate that calcipotriol and dexamethasone, in combination, synergistically suppressed the expression of IL-36α/γ, IL-23, and IL-17 in the established mouse psoriasis. Our findings indicate that the combination of calcipotriol and corticosteroid efficiently disrupts the IL-36 and IL-23/IL-17 positive feedback loop, thus revealing a mechanism underlying the superior efficacy of calcipotriol and corticosteroid combination therapy for psoriasis.

Introduction

Psoriasis is one of the most common, complex chronic inflammatory skin disorders, affecting 1%–3% of the worldwide population (1, 2). In its most common form, plaque psoriasis (PP; or psoriasis vulgaris) manifests as plaques of red, scaly, and well-demarcated regions of inflamed skin. Histologically, it is characterized by a thickening of the epidermis, with altered proliferation and differentiation of keratinocytes (KCs), and a skin infiltration of immune cells including neutrophils, DCs, and T cells (1). In addition, patients with psoriasis also exhibit signs and symptoms of systemic inflammation, resulting in an increased risk for multiple comorbid conditions, including polyarthritis, cardiovascular pathologies, and metabolic syndrome (3). Even though the mechanisms underlying the complex pathogenesis of psoriasis have not been fully elucidated, there is increasing evidence that the IL-23/IL-17 cytokine axis plays a pivotal role in the inflammatory response in psoriasis (1, 4, 5). It has been recognized that IL-23 secreted by DCs and monocytes/macrophages promotes IL-17–producing T cells, including Th17 cells and $\gamma\delta^+$ T cells, which exert pleiotropic effects on the recruitment and activation of other immune cells, such as neutrophils, as well as the hyperplasia of KCs. More recently, an elevated expression of IL-36 cytokines has been found in epidermal KCs of human psoriatic lesional skin (6–9), and IL-36 cytokines have been proposed to be a psoriasis signature (10–12). Mouse studies have also pointed out a key role for IL-36 signaling in driving and amplifying psoriatic inflammation together with IL-23/IL-17 cytokine axis (11, 13–17).

Topical therapies including corticosteroids and vitamin D3 analogues have been used for most patients with mild to moderate PP (1, 18). However, long-term corticosteroid treatments are limited by their side effects.

Authorship note: BG and RW contributed equally to this work.

Conflict of interest: The authors have declared that no conflict of interest exists.

Submitted: July 6, 2018
Accepted: December 6, 2018
Published: January 24, 2019

Reference information:
JCI Insight. 2019;4(2):e123390.
https://doi.org/10.1172/jci.insight.123390.

Since early 1990s, topical vitamin D3 analogues, such as calcipotriene or calcipotriol (Cal), have been widely used for PP; they are effective in about 45% patients and do not exhibit debilitating effects upon long-term treatment (1, 19). It has been assumed that Cal inhibits the proliferation and enhances the differentiation of KCs, as well as exerts some immunomodulator effects (19), but the underlying antipsoriasis mechanisms remain to be elucidated. Recently, a combined Cal/betamethasone treatment has been used for PP and has proved to be more efficacious than either one of these 2 agents (20, 21). Based on these clinical data, our present study was aimed to elucidate how Cal, of its own or in combination with corticosteroids, regulates the IL-23/IL-17 inflammatory axis in psoriasis, with the ultimate goal of developing more potent, better targeted, and safer treatments.

To this aim, we employed an experimental mouse model in which a psoriasis-like pathology is induced by a topical skin treatment with Aldara (Ald) cream, which contains imiquimod (IMQ) and is currently used in clinic to treat genital and perianal warts, actinic keratosis, and superficial basal cell carcinoma. Since the first report showing that topical Ald treatment induces psoriasis-like skin in mice (22), it has been widely used to create a psoriasis model (see reviews; refs. 23, 24). The relevance of this model to human psoriasis was supported by the frequent clinical incidence of psoriasis upon Ald treatment of cutaneous keratosis (23, 25). Indeed, the inflammation that is induced by topical application of Ald to mouse ears or shaved back skin of mice shows the similarities with human psoriasis and the cytokine expression (23). Particularly, Ald-induced psoriasis-like pathology is dependent on the IL-23/IL-17 axis (23). Using this model, we show in the present study that a topical treatment of Cal suppresses the IL-23/IL-17 inflammatory axis in Ald-induced mouse psoriatic skin. Importantly, by using mutant mice selectively ablated for the vitamin D receptor (VDR) in epidermal KCs, we demonstrate that this suppressive effect of Cal is mediated through keratinocytic VDR. This has led us to uncover a mechanism showing that Cal acts on KCs instead of immune cells (such as T cells, DCs, or Langerhans cells [LCs]; refs. 26, 27) to suppress the IL-23/IL-17 inflammatory axis in psoriasis and, furthermore, to provide evidence about how the combination of Cal and dexamethasone (Dex) effectively disrupt the positive cytokine feedback loop of IL-36 and IL-23/IL-17, which we believe underlies the superior efficacy of the combination therapy for psoriasis.

Results

Topical Cal inhibits the IL-23/IL-17 axis and the neutrophil infiltration in mouse psoriatic skin. Balb/c WT mouse ears were treated daily with Ald from day 0 (D0) to D4 to induce a psoriasis-like skin inflammation and were cotreated with either Cal or ethanol (ETOH, the vehicle for Cal) (Figure 1A). H&E-stained sections from Ald+ETOH ears showed an increased epidermal and dermis thicknesswith a heavy dermal cell infiltration; in contrast, Ald+Cal ears exhibited an attenuated dermal infiltration of inflammatory cells, as well as a decrease in the epidermal and dermal thickness (Figure 1B and Supplemental Figure 1A; supplemental material available online with this article; https://doi.org/10.1172/jci.insight.123390DS1). In contrast, Ald+Cal ears exhibited an attenuated dermal infiltration of inflammatory cells, as well as a decrease in the epidermal and dermal thickness (Figure 1B and Supplemental Figure 1A). Infiltration of neutrophils, one of the manifestations of a psoriasis skin inflammation, was observed in Ald+ETOH dermis (shown by NIMP-R14 staining, Figure 1B), whereas it was much lower in Ald+Cal dermis, indicating that Cal treatment suppresses the skin neutrophil infiltration.

In agreement with previous reports (see review; ref. 23), the Ald topical treatment induced the expression of IL-23p19, IL-23/12p40, IL-17A, and IL-22, as well as the calcium binding proteins S100A7A and S100A8 in skin, which are all characteristic features for psoriatic inflammation (Figure 1C). Strikingly, when mouse ears were cotreated with Cal, the induction of all of these genes was decreased (Figure 1C, compare Ald+Cal with Ald+ETOH), in keeping with a lesser infiltration of neutrophils in Ald+Cal skin (Figure 1B). Note also that the expression level of these genes in WT skin was similar between Cal and ETOH treatments, indicating that a Cal treatment did not impact the basal level of these genes. However, the expression of thymic stromal lymphopoietin (TSLP) was induced upon Cal treatment, as we previously reported (28, 29) (Figure 1C). IHC staining with an antibody against IL-23p19 confirmed that very few IL-23p19$^+$ cells were detected in the dermis from either ETOH- or Cal-treated skin (Figure 1B). In contrast, numerous IL-23p19$^+$ cells were observed in Ald+ETOH skin, most of which were located in the dermis, in agreement with the previous reports showing that dermal DCs and monocytes/macrophages are major cellular sources of IL-23 induced by IMQ/TLR7 signaling in Ald-treated skin (15, 30, 31). The increase in IL-23p19$^+$ cells was abolished in Ald+Cal skin (Figure 1B), which confirmed the data from quantitative PCR (qPCR) analyses (Figure 1C).

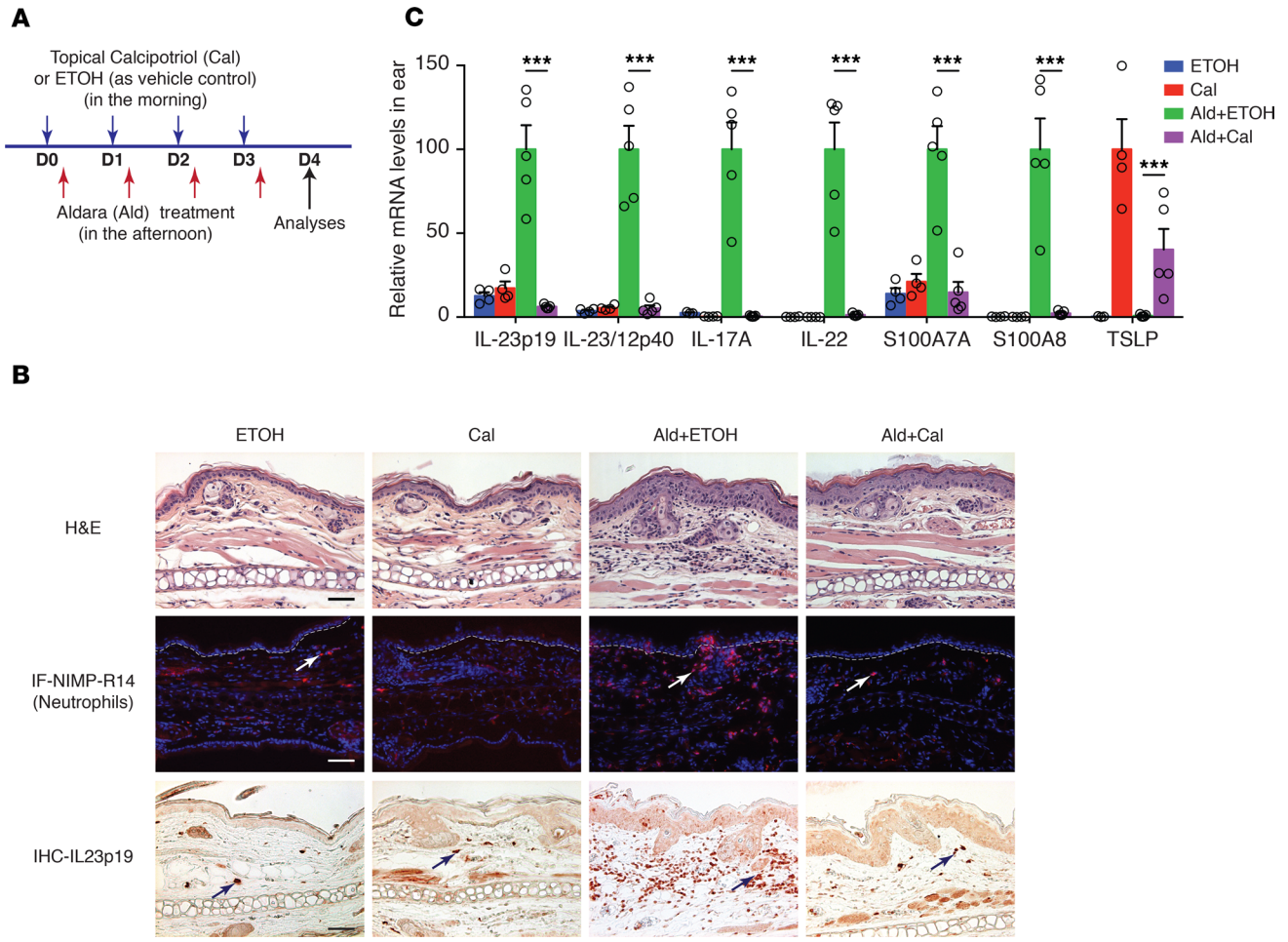

Figure 1. Topical calcipotriol inhibits the IL-23/IL-17 axis and neutrophilia in Aldara-treated skin. (**A**) Experimental protocol. WT Balb/c mouse ears were topically treated with ETOH (vehicle control), calcipotriol (Cal), Aldara (Ald)+ETOH or Ald+Cal every day from day 0 (D0) to D3, with ETOH or Cal treatment in the morning and Ald treatment in the afternoon. Mouse ears were analyzed at D4. (**B**) H&E, immunofluorescent staining with NIMP-R14 antibody (for neutrophils; red corresponds to positive signal, whereas blue corresponds to DAPI staining of nuclei), and IHC staining with IL-23p19 antibody (in dark red) of ear sections. Arrows point to positive signals. White dashed lines indicate the dermal/epidermal junction. Scale bar: 50 μm for all pictures. (**C**) qPCR analyses. Relative RNA levels were calculated using HPRT as internal control. Values are mean ± SEM. ***$P < 0.001$ (2-tailed Student's *t* test). Data are representative of 3 independent experiments with similar results.

Taken together, these results indicate that a topical Cal treatment inhibits the IL-23/IL-17 axis and the neutrophil infiltration in mouse psoriatic skin.

Keratinocytic VDR mediates the inhibition of the IL-23/IL-17 axis and neutrophilia by Cal. Next, we examined whether the inhibitory effect of Cal on the IL-23/IL-17 axis is mediated through VDR (32). $Vdr^{-/-}$ and WT littermate mice (all in Balb/c genetic background) were subjected to ETOH, Cal, Ald+ETOH, and Ald+Cal treatment, as described in Figure 1A. qPCR analyses of ears showed that, in $Vdr^{-/-}$ mice, Cal failed to inhibit the Ald-induced expression of IL-23p19, IL-23/IL-12p40, IL-17A, IL-22, S100A7A, and S100A8 (Figure 2A), indicating that the inhibition of IL-23/IL-17 by Cal is indeed mediated via VDR. As expected (29), the induction of TSLP by Cal was VDR dependent (Figure 2A).

As VDR is expressed in numerous skin cell types, including KCs, we then asked whether the inhibition of IL-23/IL-17 by Cal could be mediated through keratinocytic VDR. To this end, mice with the ablation of VDR selectively in epidermal KCs (K14-$Cre^{tg/0}$/$Vdr^{L2/L2}$ mice, called here after $Vdr^{KC-/-}$ mice) (29) were subjected to ETOH, Ald+ETOH, or Ald+Cal treatment as described in Figure 1A. Interestingly, Cal failed to inhibit the Ald-induced IL-23/IL-17 axis in $Vdr^{KC-/-}$ mice (Figure 2B), and it was not able to reduce the dermal infiltrate in Ald-treated $Vdr^{KC-/-}$ mice (Figure 2C; H&E staining). IHC staining with IL-23p19 antibody, as well as immunofluorescent (IF) staining with NIMP-R14 antibody, showed that Cal treatment could not reduce the number of IL-23p19$^+$ cells and neutrophils in $Vdr^{KC-/-}$ dermis (Figure 2C).

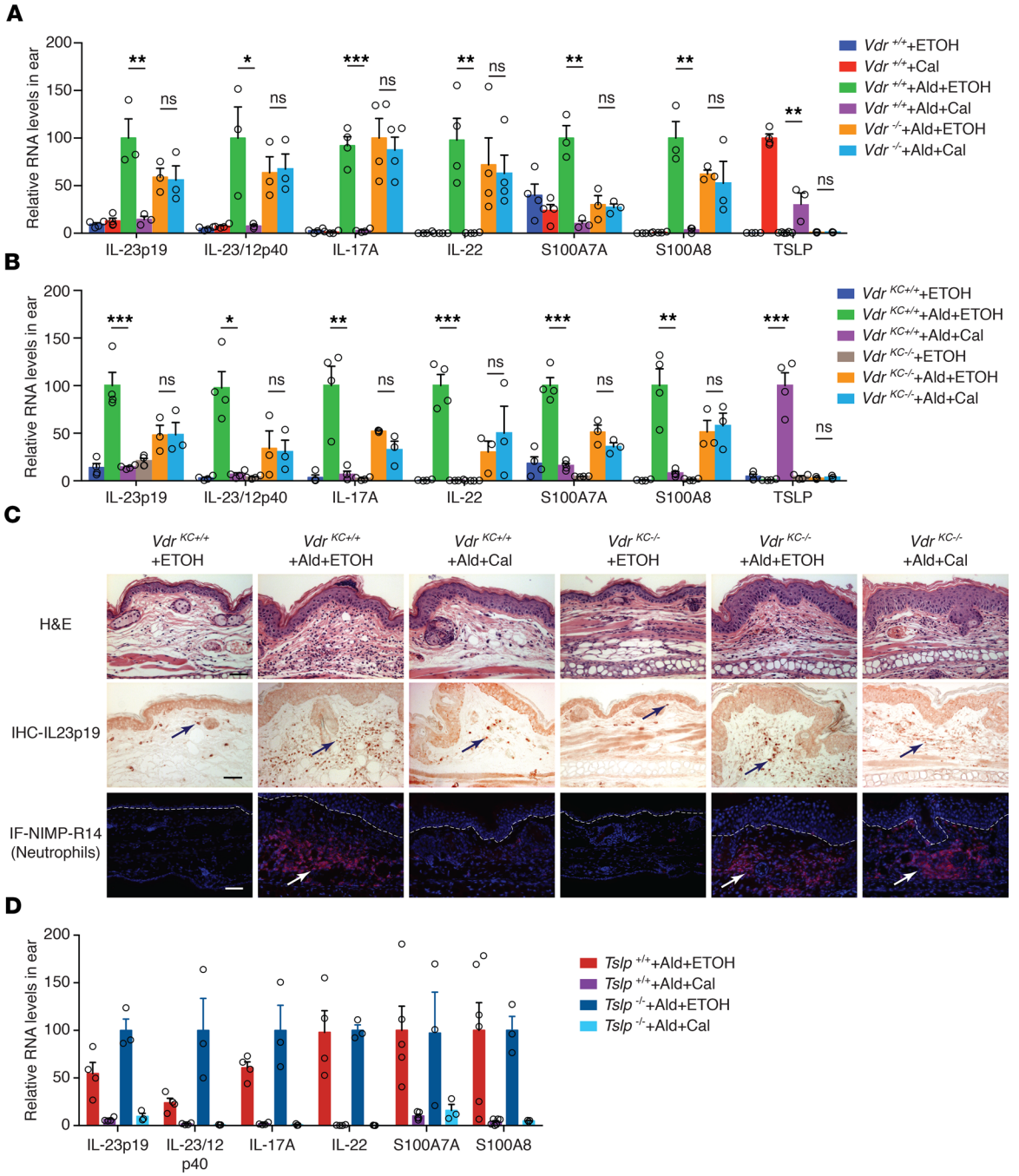

Figure 2. Keratinocytic VDR mediates the inhibition of IL-23/IL-17 and neutrophilia by calcipotriol in mouse psoriatic skin. (**A** and **B**) $Vdr^{-/-}$ mice and their littermate $Vdr^{+/+}$ mice (**A**), $Vdr^{KC-/-}$ mice ($K14\text{-}Cre^{Tg/0}/Vdr^{L2/L2}$) and their littermate $Vdr^{KC+/+}$ controls ($K14\text{-}Cre^{0/0}/Vdr^{L2/L2}$) (**B**) were treated with ETOH, calcipotriol (Cal), Aldara (Ald)+ETOH, or Ald+Cal, as described in Figure 1A. Ears were analyzed by qPCR at D4. $^{*}P < 0.05$; $^{**}P < 0.01$; $^{***}P < 0.001$ (2-tailed Student's *t* test). Values are mean ± SEM. (**C**) H&E staining, IHC staining with IL-23p19 antibody (in dark red), and immunofluorescent (IF) staining with NIMP-R14 antibody (for neutrophils; red corresponds to positive signal, whereas blue corresponds to DAPI staining of nuclei) among $Vdr^{KC+/+}$ and $Vdr^{KC-/-}$ ear sections. White dashed lines indicate the dermal/epidermal junction. Scale bar: 50 μm. (**D**) qPCR analyses of ears from $Tslp^{-/-}$ mice and their littermate $Tslp^{+/+}$ mice treated with ETOH, Cal, Ald+ETOH, or Ald+Cal, as described in Figure 1A. Ears were analyzed by qPCR at D4. Values are mean ± SEM. Data are representative of 3 independent experiments with similar results.

Together, these data demonstrate that the suppression of the psoriatic inflammation by Cal is dependent on keratinocytic VDR. Note that, as KCs do not express TLR7 either in mice (15) or humans (33, 34) (Supplemental Figure 2), our results do not seem to reflect a crosstalk between VDR signaling and TLR7 signaling in KCs; instead, our data suggest that the Cal/VDR signaling most likely regulates

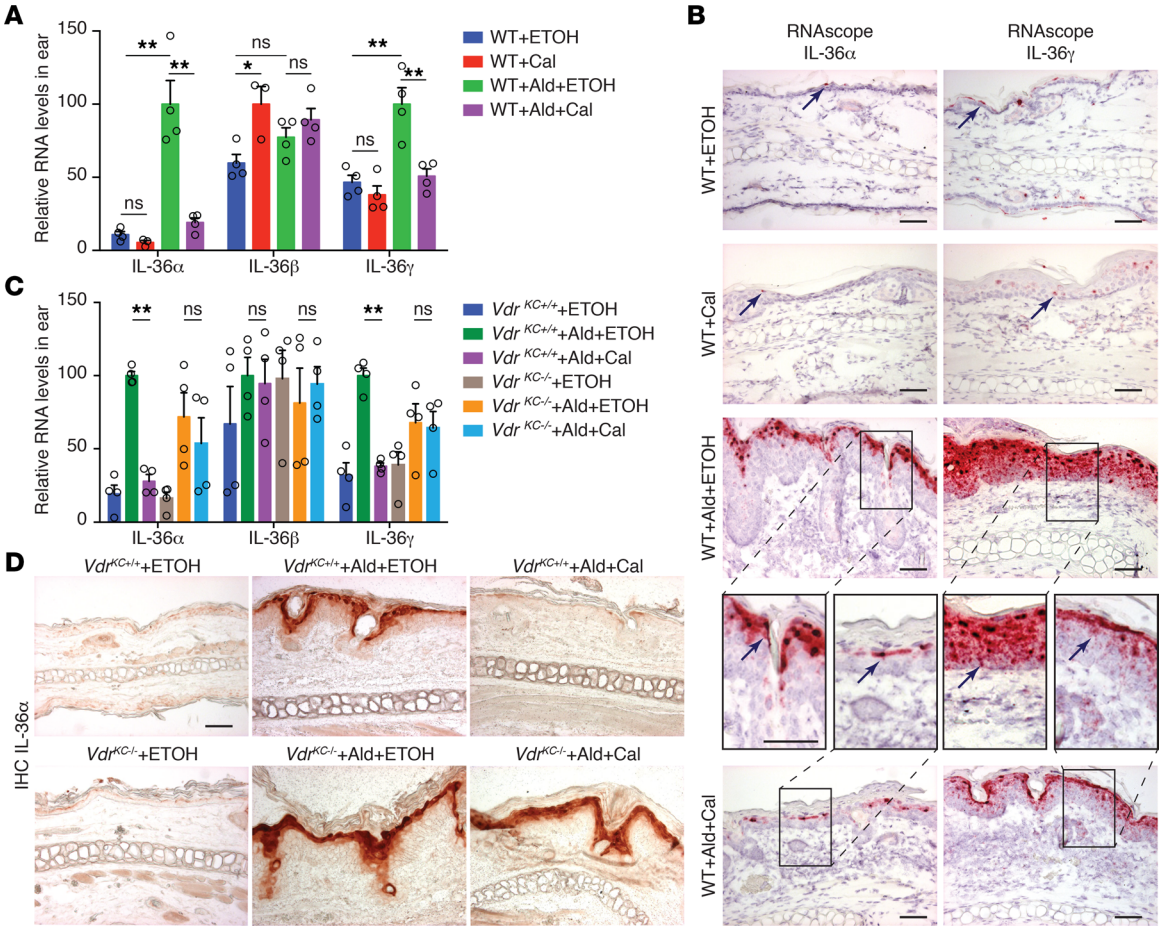

Figure 3. Calcipotriol inhibits IL-36α/γ expression in mouse psoriatic skin epidermis in a keratinocytic VDR-dependent manner. (**A**) qPCR analyses for IL-36 in Balb/c WT ears treated with ETOH, Cal, Ald+ETOH, or Ald+Cal (as described in Figure 1A). $*P < 0.05$; $**P < 0.01$ (2-tailed Student's *t* test). Values are mean ± SEM. (**B**) RNAscope in situ hybridization with IL-36α or IL-36γ probe (signals are in red) on mouse ear sections, counterstained with hematoxylin. Scale bar: 50 μm. (**C**) qPCR analyses for IL-36 in $Vdr^{KC-/-}$ mice ($K14\text{-}Cre^{Tg/0}/Vdr^{L2/L2}$) and their littermate $Vdr^{KC+/+}$ controls ($K14\text{-}Cre^{0/0}/Vdr^{L2/L2}$), treated with ETOH, Ald+ETOH, or Ald+Cal. Values are mean ± SEM. $**P < 0.01$ (2-tailed Student's *t* test). (**D**) IHC staining with IL-36α antibody on ear sections. Positive cells are in dark red. Scale bar: 50 μm. Data are representative of 3 independent experiments with similar results.

certain factors, such as cytokines produced and released by KCs, which consequently regulates a IL-23/IL-17 cascade in immune cells.

We initially hypothesized that the cytokine TSLP produced by mouse KCs mediated the inhibition of the IL-23/IL-17 axis, as Cal is known to induce TSLP overexpression in mouse KCs, thereby driving a Th2 immune response (28, 29, 35, 36), which may counter-regulate the IL-23/IL-17 axis (37). However, when subjected to a Cal treatment, $Tslp^{-/-}$ mice exhibited a similar reduction in Ald-induced expression of IL-23p19, IL-23/IL-12p40, IL-17A, IL-22, S100A7A, and S100A8 as WT $Tslp^{+/+}$ mice (Figure 2D), thus indicating that KC-derived factors other than TSLP are involved in the inhibition of the IL-23/IL-17 axis by Cal.

Cal inhibits IL-36α and IL-36γ expression in mouse psoriatic skin. Evidence has been provided indicating that IL-36 cytokines play a key role in driving and maintaining psoriatic inflammation. Indeed, an elevated expression of IL-36α, IL-36β, or IL-36γ has been reported in human psoriatic lesional skin (6, 7, 9, 11, 12); furthermore, mutations of the IL36RN gene that encodes IL-36 receptor antagonist, leading to an enhanced IL-36 signaling, were associated with generalized pustular psoriasis patients (38, 39). Furthermore, it was shown that IL-36R–deficient mice, as well as mice with blockade of IL-36R, were protected from the Ald-induced IL-23/IL-17/IL-22 axis and psoriasis disease development (11, 13, 15). More recently, it was reported that mice with ablation of IL-36α (but not IL-36β or IL-36γ) failed to develop psoriasis upon Ald treatment (14). We therefore examined whether the Ald-induced IL-36 expression could be modulated by Cal. qPCR analyses showed that IL-36α and IL-36γ, but not IL-36β, were significantly induced in ears from WT mice with Ald+ETOH treatment as compared with those with ETOH treatment (Figure 3A), in agreement with a

previous report using the Ald model (6). Strikingly, the expression of IL-36α and IL-36γ was greatly diminished in Ald+Cal ears, whereas IL-36β mRNA levels remained unchanged (Figure 3A). Of note, skin treated with WT+Cal and WT+ETOH did not exhibit significant difference in RNA levels of IL-36α and IL-36γ, although a tendency of decrease could be seen in WT+Cal skin (Figure 3A).

We next examined the location of IL-36α– or IL-36γ–expressing cells in Ald-treated skin, using RNAscope in situ hybridization, an assay which exhibits high specificity and sensitivity. In either WT+ETOH or WT+Cal ears, IL-36α was barely detected, while some positive cells for IL-36γ could be seen in the epidermis (Figure 3B). In WT+Ald+ETOH skin, there was a strong increase of IL-36α signal, which was specifically located in the outmost suprabasal layer of epidermis (Figure 3B, left panel). IL-36γ was also induced, but throughout all layers of epidermis, while weaker signals could be seen in the dermis (Figure 3B, right panel). In WT+Ald+Cal ears, the expression of IL-36α and IL-36γ was diminished in the epidermis, whereas IL-36γ signals in the dermis remained unchanged (Figure 3B). These results indicate that Ald induces IL-36α and IL-36γ transcripts located in suprabasal layer and all layers in epidermis, respectively — both of which are downregulated upon Cal treatment.

We then investigated whether the inhibition of Ald-induced IL-36α and IL-36γ by Cal could be mediated through keratinocytic VDR. qPCR results showed that, in $Vdr^{KC-/-}$ mice, Cal failed to downregulate the Ald-induced IL-36α and IL-36γ expression (Figure 3C). To validate these results at the protein level, we performed IHC staining with an IL-36α antibody (a specific antibody against mouse IL-36γ was not available). IL-36α was very weakly detected in ETOH-treated $Vdr^{KC+/+}$ and $Vdr^{KC-/-}$ mice, whereas it was strongly induced in the suprabasal layer of epidermis of both $Vdr^{KC+/+}$ and $Vdr^{KC-/-}$ mice upon Ald+ETOH treatment (Figure 3D). Upon Ald+Cal treatment, the IL-36α signal was greatly decreased in $Vdr^{KC+/+}$ but not in $Vdr^{KC-/-}$ epidermis, demonstrating that Cal inhibits the IL-36α protein production in the suprabasal layer of the epidermis, which is mediated through the keratinocytic VDR.

As it was recently described that, among various mouse strains, Ald response in C57BL/6J (B6) mice were mostly consistent with human psoriasis (40), we further examined whether Cal had a similar effect in Ald-treated B6 mice, as we observed with Balb/c mice. Our kinetic analyses showed that the development of psoriatic inflammation was relatively delayed in B6 mouse ears compared with Balb/c, as a similar skin inflammation was observed at D6 (with 6× Ald) for B6 mice and at D4 (with 4× Ald) for Balb/c mice (Supplemental Figure 3A), in good agreement with what was previously reported (22). Nevertheless, our results confirmed that topical Cal treatment inhibited skin inflammation in Ald-treated B6 mouse ears (Supplemental Figure 3, B and C; compare [(6×Ald)+(6×Cal)] and [(6×Ald)+(6×ETOH)]); moreover, Cal treatment reduced the Ald-induced expression of IL-23p19, IL-23p40, IL-17A, and IL-22, as well as IL-36α/γ in B6 mouse ears (Supplemental Figure 3, D and E), in a similar way as observed in Balb/c mice.

Topical treatment of Cal downregulates IL-36α/γ expression in human psoriasis skin. To explore the human relevance of our findings from mouse models, 4 patients with PP received topical treatment of Cal (Daivonex cream) once per day for 4 days, and biopsies performed before and after treatment on the same lesion were analyzed by qPCR. Results showed that the mRNA expression of human IL-36α (hIL-36α) and hIL-36γ, but not hIL-36β, was highly elevated in all of the 4 PP skin as compared with healthy skin (HS) (Figure 4). This was correlated with the increase of hIL-23p19, hIL-17A, and hIL-22 in PP skin and, to a lesser extent, with hIL-23/hIL-12p40 — but not with hIL-12p35. The level of hTSLP in PP skin showed a mild increase as compared with HS. Most interestingly, upon the 4-day Cal treatment, the levels of hIL-36α, hIL-36γ, hIL-23p19, and hIL-23/12p40, as well as hIL-17A, were all decreased in 3 of the 4 patients (i.e., in patient nos. 1, 2, and 4), while patient no. 3 did not respond to the Cal treatment. Indeed, qPCR analysis of hCyp24A1, a gene known to be positively regulated by vitamin D3, showed that hCyp24A1 was induced upon Cal treatment in patient nos. 1, 2 and 4, but not in the patient no. 3 (Figure 4). We conclude from these results that, in agreement with our mouse data, a Cal treatment reduces the expression of hIL-36α, hIL-36γ, hIL-23p19, hIL-23/12p40, and hIL-17A in human psoriasis skin. The exceptions were for IL-22, which was reduced in only 2 of the 4 patients upon Cal treatment, and for TSLP, whose expression was not upregulated by Cal, in contrast with what was observed in mouse skin (Figure 1C and refs. 28, 29).

Cal, but not Dex, inhibits IL-36α/γ expression in Ald-treated immunodeficient NSG mice. In addition to vitamin D derivatives, topical corticosteroids have been used for therapy of mild to moderate psoriasis (1, 18). Topical treatment with Dex ameliorated the Ald-induced skin inflammation (Figure 5A, upper panel) and reduced the expression of IL-23p19, IL-23/12 p40, IL-17A, and IL-22 (Figure 5B). These observations

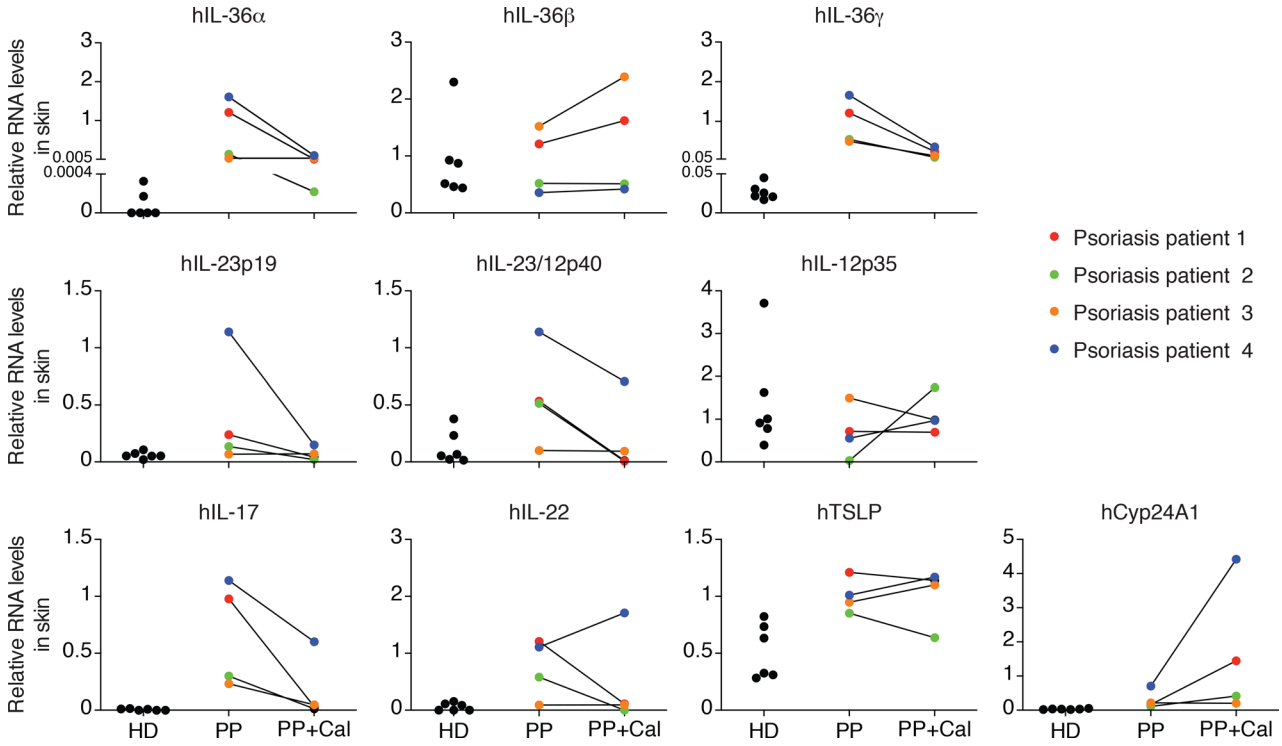

Figure 4. Topical treatment of calcipotriol downregulates hIL-36α and hIL-36γ expression in human psoriasis skin. Skin biopsies were taken from healthy donors (HD), or from lesional skin of plaque psoriatic patients (PP) before and after a 4-day topical treatment with Calcipotriol ointment (DAIVONEX) once a day, and qPCR analyses were performed. Individual values are shown, with the line connecting paired samples from the same patient before and after the calcipotriol treatment.

were in keeping with previous studies showing that Dex inhibited IL-23 expression from DCs (26) or macrophages (41), as well as IL-17/IL-22 expression by T cells (26). Interestingly, we found that the levels of IL-36α and IL-36γ in skin were also reduced (Figure 5B), but such reduction was less prominent as compared with Cal treatment (Figure 3A). IHC staining confirmed that, in WT skin treated with Ald+Dex, IL-36α signals in the suprabasal layer of epidermis were decreased (Figure 5A, lower panel); however, the remaining IL-36α signal in Ald+Dex skin was higher as compared with Ald+Cal skin, in which IL-36α expression was nearly abolished (Figure 3D).

It has been shown that IL-36 cytokines initiate and promote the expression of IL-17/IL-22, but the latter can also induce IL-36 cytokine expression, suggesting a positive feedback regulation loop between IL-36 and IL-17/IL-22 (9, 42). We wondered whether Cal, Dex, or both actually inhibit the expression of IL-36α/γ in a direct manner in KCs. To explore these possibilities, we employed the immunodeficient Nod-Scid *Il2rg*–/– (NSG) mouse line, which lacks T cells, B cells, NK cells, and innate lymphoid cells (ILCs) (43). Ald-treated NSG mice did not exhibit an immune infiltrate in dermis (Figure 5C, upper panel), nor any expression of IL-17 and IL-22, due to the absence of cells producing these cytokines, including Th17 cells, γδ T cells, and ILCs (Figure 5D). However, RNA levels of IL-36α and IL-36γ were significantly increased (compare NSG+Ald+ETOH with NSG+ETOH). IHC staining confirmed an increase of the IL-36α signal in the suprabasal layer of the epidermis of NSG mice treated with Ald+ETOH (Figure 5C, lower panel; compare NSG+Ald+ETOH with NSG+ETOH). Notably, the increase in IL-36α/γ (but not IL-36β) in NGS mice was lower when compared with WT mice, as shown by qPCR analyses (Figure 5D) or IHC for IL-36α (compare Figure 5C with Figure 3D). These results indicate that the expression of IL-36α/γ is directly induced by Ald in the absence of IL-17/IL-22 and that their expression is reinforced by IL-17/IL-22.

We then employed Ald-treated NSG mice to examine whether the inhibition of IL-36α/γ by Cal or Dex was a direct effect on KCs, or an indirect effect subsequent to the decrease in IL-17/IL-22. As shown in Figure 5, C and D, Ald-induced expression of IL-36α and IL-36γ was inhibited by Cal (compare NSG+Ald+Cal with NSG+Ald+ETOH). However, Dex did not have any effect on the expression

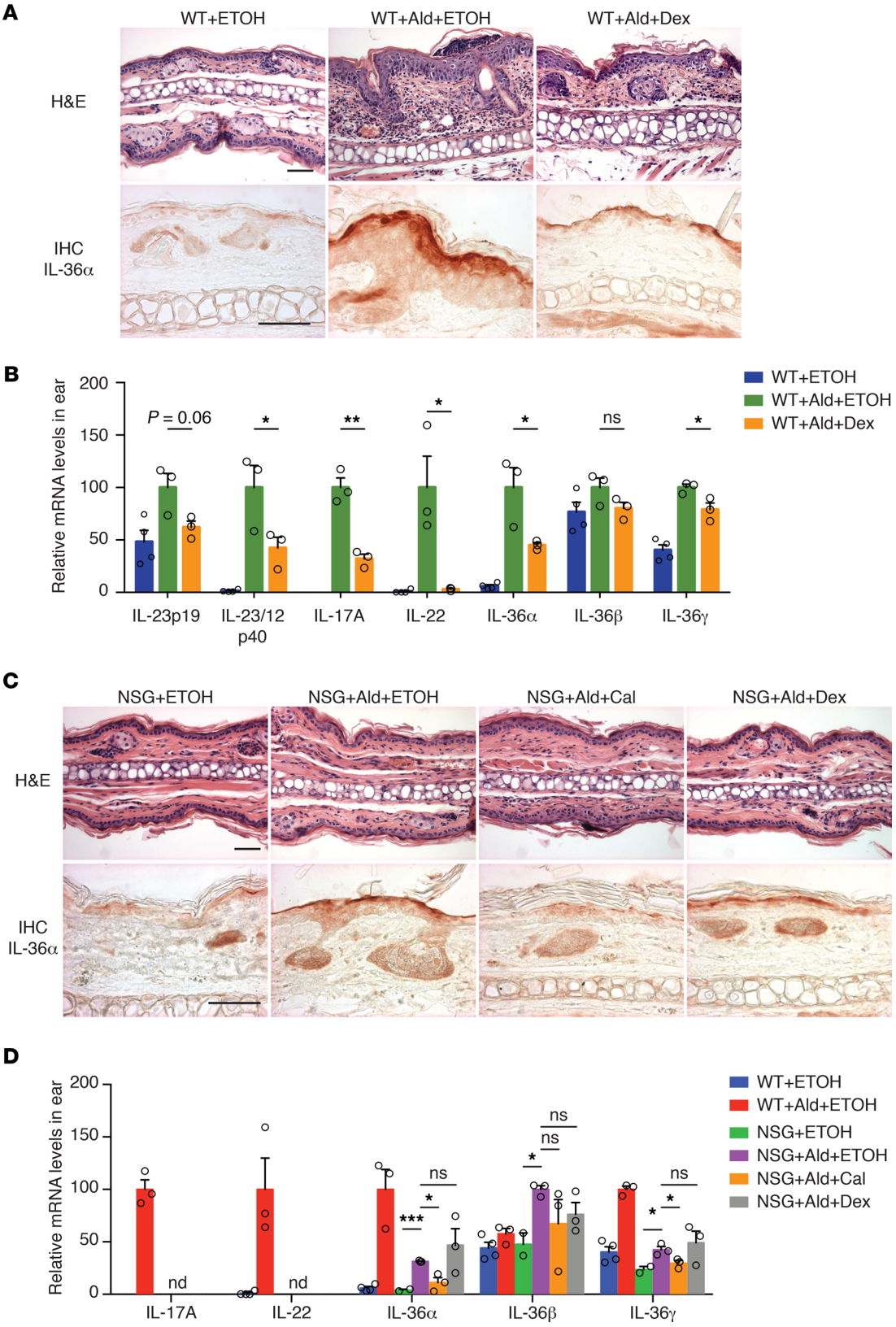

Figure 5. Calcipotriol directly suppresses the expression of IL-36α/γ in mouse skin, but the effect of dexamethasone is indirect. (**A** and **B**) Topical dexamethasone (Dex) reduces IL-23/IL-17/IL-22 as well as IL-36α/γ expression in mouse psoriatic skin. WT Balb/c mouse ears were topically treated with ETOH, Aldara (Ald)+ETOH, or Ald+Dex from day 0 (D0) to D3, with ETOH or Dex in the morning and Ald in the afternoon, as shown in Figure 1A. Ears were analyzed at D4. (**A**) H&E staining (upper panel) and IHC staining with IL-36α antibody (lower panel; positive signals are in dark red). Scale bar: 50 μm. (**B**) qPCR analyses of ears. Values are mean ± SEM. $^{*}P < 0.05$; $^{**}P < 0.01$ (2-tailed Student's *t* test). Data are representative of 3 independent

experiments with similar results. (**C** and **D**) Calcipotriol but not dexamethasone inhibits IL-36α/γ in Aldara-treated immunodeficient NSG mouse ears. (**C**) H&E staining (upper panel) and IHC staining with IL-36α antibody (lower panel; positive signals are in dark red). Scale bar: 50 μm. (**D**) qPCR analyses of the treated ears. nd, not detected. Values are mean ±SEM. $*P < 0.05$; $***P < 0.001$ (2-tailed Student's *t* test). Data are representative of 2 independent experiments with similar results.

of IL-36α or IL-36γ in Ald-treated NSG mice (compare NSG+Ald+Dex with NSG+Ald+ETOH). Taken together, these data suggest that the Cal treatment directly inhibits the expression of IL-36α/γ in KCs, whereas Dex treatment indirectly leads to the reduced expression of IL-36α/γ via the suppression of IL-23/IL-17/IL-22 in immune cells.

Cal represses IL-36α/γ expression in mouse epidermal KCs and human primary KCs. To further support that Cal directly regulates the expression of IL-36α and IL-36γ in epidermal KCs, the epidermis of WT Balb/c mouse ears was separated from the dermis, and an ex vivo culture of epidermal sheet was carried out in the presence of Cal or Dex. A significant decrease in IL-36α and IL-36γ expression was observed in the presence of Cal but not of Dex (Figure 6A, left panel). Moreover, this repression was abolished in ex vivo–cultured epidermis from $Vdr^{KC-/-}$ mice (Figure 6A, right panel), indicating that the transcriptional repression of IL-36α/γ by Cal is mediated by keratinocytic VDR.

We next examined whether Cal may repress the expression of both IL-36α and IL-36γ in human KCs. In freshly isolated human primary KCs (HPKCs) from healthy donors, hIL-36γ — but not hIL-36α — RNA was detected by qPCR (Figure 6B; nonstimulated). We stimulated HPKCs in the presence of TNF-α, IFN-γ, and IL-17A, alone or in combination, in order to mimic the psoriatic skin microenvironment (44), and we examined the induction of hIL-36. We found that, when stimulated with either TNF-α, IFN-γ, or IL-17A alone, the expression of hIL-36γ was readily increased in HPKCs; however, hIL-36α remained undetectable (Figure 6B, healthy donor-A) or very low (Figure 6B, healthy donor-B). Among all combinations tested, the triple stimulation with TNF-α+IFN-γ+IL-17A resulted in the strongest stimulation of IL-36α and IL-36γ in both HPKCs derived from healthy donor-A and donor-B (Figure 6B).

We then added Cal or Dex to HPKCs stimulated with the mix of TNF-α+IFN-γ+IL-17A and examined by qPCR their effects on IL-36α/γ expression. Cal did repress both hIL-36α and hIL-36γ, while Dex had no effect on IL-36α expression and weakly decreased IL-36γ expression (Figure 6C). In addition, the Cal+Dex exhibited similar effect as Cal alone (Figure 6C). We conclude that, as observed in mice, Cal — but not Dex — exerts a direct repression on the expression of IL-36α and IL-36γ in human KCs.

Cal and Dex synergistically suppress the expression of IL-36α/γ in the established psoriasis in mice. During the last years, clinical studies have shown that a combined local therapy of psoriasis with Cal and corticosteroids generated the superior efficacy over use of either agent alone (20, 21). We suspected that Cal and Dex could synergistically suppress the expression of IL-36α/γ in the establish psoriatic inflammation. To test that, Balb/c WT mouse ears were first daily treated with Ald from D0 to D3 to induce a psoriatic inflammation and were then posttreated with ETOH, Cal, Dex, or Cal+Dex at D4 and D5 (Figure 7A). Histological analyses of the skin showed a decrease in dermal inflammatory infiltration in both Ald+2×Cal and Ald+2×Dex groups (as compared with Ald+2×ETOH), but most interestingly, the Ald+(2×Cal+Dex) group exhibited a further decrease in skin inflammatory infiltration (Figure 7B, H&E staining) and in thicknesses of the epidermis and the dermis (Supplemental Figure 1B). We then examined the expression of IL-36α and IL-36γ by IHC staining and RNA in situ hybridization. The Cal posttreatment suppressed the IL-36α/γ expression in the established psoriasis (Figure 7B, compare WT+Ald+2×ETOH and WT+Ald+2×Cal). The Dex posttreatment also led to a reduced level of IL-36α and IL-36γ, although this reduction is lesser than that achieved by Cal (Figure 7B). A combined treatment with Cal and Dex resulted in a synergistic suppression of IL-36α expression (as shown by both IHC staining and RNA in situ hybridization), as well as of IL-36γ expression (as shown by RNA in situ hybridization). Similarly, a synergistical reduction by Cal and Dex cotreatment was also observed for IL-23p19, IL-23/IL-12p40, IL-17A, and IL-22 in Ald-treated skin (Figure 7C). Taken together, our data indicate that a cotreatment with Cal and Dex synergistically and efficiently suppresses the expression of IL-36α/γ and IL-23/IL-17/IL-22 in the established psoriasis in mice.

Discussion

In this study, we have explored mechanisms underlying the therapeutic effects of the vitamin D3 analog Cal, on its own or in combination with Dex, in the treatment of PP. Employing an experimental mouse psoriasis model, we demonstrate that topical Cal inhibits the IL-23/IL-17 axis in psoriatic inflammation

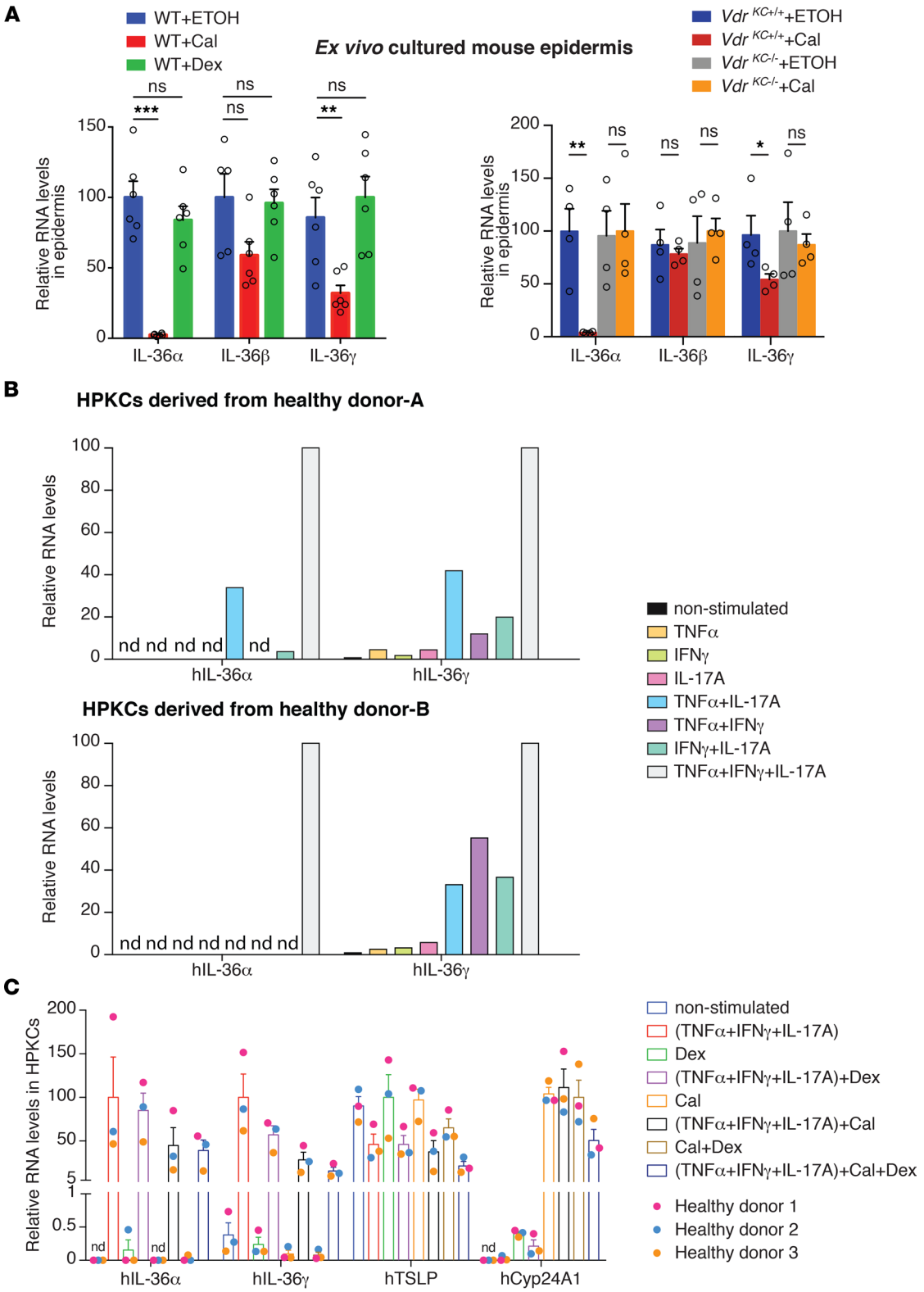

Figure 6. Calcipotriol represses IL-36α/γ expression in mouse epidermal keratinocytes and human primary keratinocytes. (**A**) Calcipotriol but not dexamethasone represses IL-36α/γ expression in ex vivo cultured mouse epidermis in a keratinocytic VDR–dependent manner. Data show the qPCR analyses of cultured epidermis from WT Balb/c mice (left panel) or from $Vdr^{KC+/+}$ and $Vdr^{KC-/-}$ mice (right panel). Values are mean ± SEM. $^{*}P < 0.05$; $^{**}P < 0.01$; $^{***}P < 0.001$ (2-tailed Student's *t* test). Data are representative of 2 independent experiments with similar results. (**B** and **C**) Calcipotriol represses IL-36α/γ expression in human primary keratinocytes (HPKCs). (**B**) HPKCs derived from 2 healthy donors were stimulated HPKCs in the presence of TNF-α, IFN-γ and IL-17A, alone or in combination, and they were examined the induction of hIL-36α and hIL-36γ. (**C**) HPKCs derived from 3 healthy donors were stimulated with cytokine cocktails (TNF-α+IFN-γ+IL-17A), in combination with calcipotriol (Cal), dexamethason (Dex), or both for 24 hours, and gene expression was analyzed by qPCR. Dots with the same color (red, blue, or orange) represent HPKCs derived from the same donor no. 1, 2, or 3.

via keratinocytic VDR signaling. We reveal that Cal directly represses the expression of IL-36α and IL-36γ in mouse epidermal KCs, and we show that this mechanism is conserved in humans. In contrast with Cal, we find that Dex does not directly repress IL-36α/γ expression in mouse or human KCs; however, the topical treatment of Dex indirectly decreases IL-36α/γ in KCs. Furthermore, we obtain evidence indicating that the concomitant suppression of IL-36α/γ by Cal in KCs and of IL-23/IL-17 by Dex in immune cells efficiently interrupt the positive feedback loop of IL-36α/γ and IL-23/IL-17. These results reveal a plausible mechanism for the superior efficacy of the combined Cal/corticosteroid therapy for psoriasis, which is schematically presented in Figure 8.

Our data demonstrate that Cal acts on KC to exert its antiinflammatory effect on psoriasis.. This is different from previous studies proposing that Cal acts on immune cells to modulate IL-23/IL-17 inflammation. For example, it was shown that Cal acted on DCs and T cells in ex vivo–cultured human psoriatic skin explants to inhibit IL-23 and IL-17 expression, respectively (26). More recently, it was reported that Cal suppressed the IL-23 expression by epidermal LCs, which was assumed to be the reason for the inhibition of IL-17 by Cal in Ald-induced mouse psoriasis (27). In our study, we showed that the inhibition of IL-23/IL-17/IL-22 by Cal was abolished in $Vdr^{KC-/-}$ (mice with the ablation of VDR selectively in KCs) (Figure 2, A and B), which demonstrates that this inhibiting effect is actually dependent on keratinocytic VDR. As to IL-23, our IHC staining showed that IL-23$^+$ signals were predominantly detected in dermis but not in epidermis of Ald-treated mouse skin (Figure 2C). This result suggests that Cal inhibits IL-23, which is expressed by dermal DCs or/and monocytes/macrophages, in keeping with other studies suggesting that Langerin-negative dermal conventional DCs (cDCs) produce IL-23 to drive psoriatic inflammation (31) and that LCs have no essential role — or rather an antiinflammatory role — in psoriatic inflammation (45–47).

Recent studies have provided compelling evidence that IL-36 signaling plays a key role in driving and amplifying psoriatic inflammation. Particularly, mice deficient of IL-36R or mice with blockade of IL-36R were protected from the Ald-induced IL-23/IL-17 axis and disease development (11, 13, 15); on the other hand, IL-36R antagonist–deficient ($Il36rn^{-/-}$) mice showed exacerbated pathologies (15). More recently, it has been also shown that IL-36γ induces IL-23 production from psoriasis macrophages (16) and that IL-36α promotes DC-induced Th17 differentiation (17) or directly induces IL-17 on CD4$^+$ T and γδ T cells (48). Of note, we observed that, in contrast with IL-36α and IL-36γ, IL-36β was not significantly induced in either mouse (Figure 3A) or human (Figure 4) psoriatic skin. A similar observation was made by a recent study from Boutet et al. (6), although others reported that IL-36α, -β, and -γ were all induced in human psoriasis (8, 9, 49). Nevertheless, Cal did not repress the expression of IL-36β in either mouse or human psoriatic skin. Therefore, different from IL-36α/γ, IL-36β appears to be neither associated with the IL-23/IL-17 axis in psoriasis nor related to the antiinflammatory effect of Cal.

However, our data do not distinguish whether IL-36α, IL-36γ, or both are primary targets of Cal for its antipsoriasis effect. These 2 cytokines appear to be closely associated in psoriatic inflammation and to be able to interregulate each other (i.e., one induces another) (50, 51). Interestingly, IL-36α was recently suggested to play a primary role in psoriasis pathogenesis, as mice with ablation of IL-36α, but not (or to a much lesser extent) of IL-36β or IL-36γ, failed to develop Ald-induced psoriasis (14). Indeed, despite the fact that IL-36α and IL-36γ utilize the same receptor (IL-36R/IL-1RacP), IL-36α seems to have a higher affinity than IL-36γ to both IL-36R and IL-36R/IL-1RAcP heterodimer (52); therefore, it may drive specified downstream signals. Moreover, IL-36α and IL-36γ may be differently induced in certain physiological or pathological contexts. For example, IL-36α (but not IL-36γ) was shown be promoted by epicutaneous Staphylococcus aureus (48), while IL-36γ was shown to be induced in skin injury (53). It will be interesting to determine the specified versus redundant roles of IL-36α and -γ in cytokine network and inflammatory pathways in psoriasis and other pathologies, which should provide useful information for designing specific targeting strategies.

How the expression of IL-36α/γ is repressed by Cal remains to be further investigated. In our study, we have shown that such repression requires keratinocytic VDR. However, the KO of VDR in KCs ($Vdr^{KC-/-}$) did not lead to a spontaneous upregulation of IL-36α or IL-36γ expression (Figure 3C, comparing $Vdr^{KC-/-}$+ETOH with $Vdr^{KC+/+}$+ETOH); moreover, there was no increase in IL-36α or IL-36γ expression in the Ald-treated $Vdr^{KC-/-}$ skin compared with Ald-treated WT skin (Figure 3C, comparing $Vdr^{KC-/-}$+Ald+ETOH with $Vdr^{KC+/+}$+Ald+ETOH). In other words, in the absence of Cal treatment, VDR on its own does not seem to repress the expression of IL-36α/γ. Besides Cal, we confirmed that the active

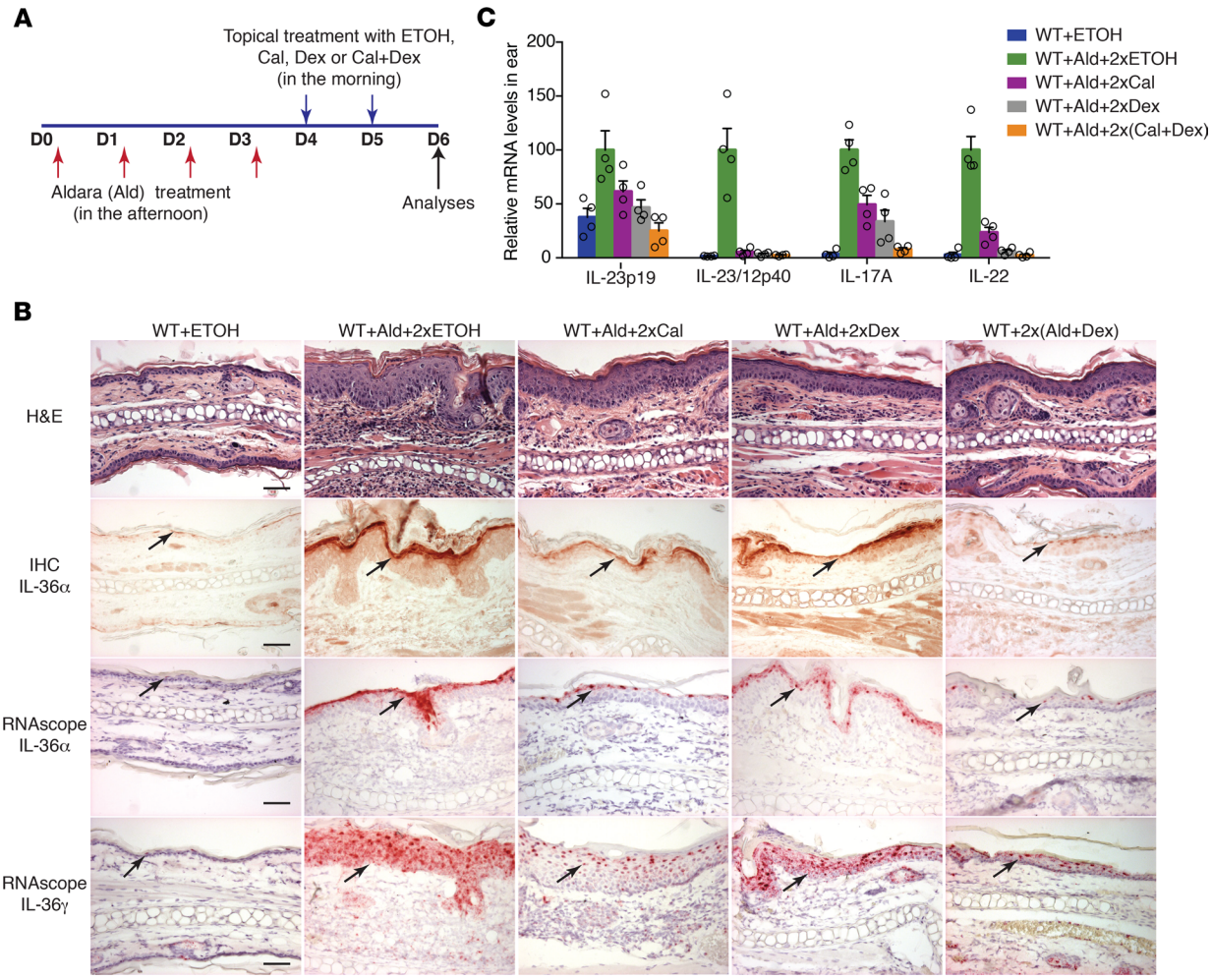

Figure 7. A synergy between calcipotriol and dexamethasone in repressing IL-36α/γ and IL-23/IL-17/IL-22 in the established psoriasis in mice. (**A**) Experimental protocol. WT Balb/c mouse ears were topically treated with Aldara (Ald) from D0 to D3 to induce psoriatic inflammation, followed by 2 times of treatment with ETOH, calcipotriol (Cal), dexamethasone (Dex), or Cal+Dex at D4 and D5. Ears were sampled for analyses at D6. (**B**) Skin sections were used for H&E staining, IHC staining with IL-36α antibody, and RNAscope in situ hybridization with probes for IL-36α or IL-36γ. Arrows point to positive signals. Scale bar: 50 μm. (**C**) qPCR analyses of the treated skin. Values are mean ± SEM. Data are representative of 3 independent experiments with similar results.

vitamin D3, 1α,25-dihydroxyvitamin D3 (calcitriol), also exerted a similar repression of Ald-induced IL-36 expression (Supplemental Figure 4, A–C). These results suggest that the repression of IL-36α/γ by Cal implicates a mechanism of ligand-dependent VDR-mediated transrepression.

Molecular mechanisms underlying the negative regulation of genes by the liganded-VDR are not well understood. Various modes of transrepression have been proposed via different types of negative vitamin D response elements (nVDRE) present in different genes, including putative DR3-type elements (54, 55). Interestingly, Jiang et al. recently identified a DR3 element as a nVDRE in a hIL-36γ promoter (53). To test whether DR3 elements could mediate the transrepression of hIL-36α, we used Find Individual Motif Occurrences (FIMO 4.10) (56) to predict VDREs (MA0693.1, JASPAR 2016) (57) in the promoter region. Within 673 bp upstream of transcription start site (i.e., 1085 bp upstream of translational start codon ATG), we identified 3 potential elements, DR3a, DR3b, and DR3c, after having filtered significant hits with $P < 0.001$ (Supplemental Figure 5A). Among these, DR3c showed the best fit ($P = 5 \times 10^{-5}$). Interestingly, by constructing firefly luciferase reporters for transient transfection to HaCaT cells, we observed that the deletion of DR3c (but not DR3a) in the hIL-36α promoter led to an abolishment of the repression by Cal (Supplemental Figure 5B), suggesting that DR3c functions as one nVDRE to mediate the negative regulation of IL-36α by liganded VDR. However, as it has been recognized that multiple response elements often exist not only in proximal, but also in distal, regions of VDR-regulated genes, our results do not exclude other nVDREs in more upstream regions of the hIL-36α promoter (Supplemental Figure 5C).

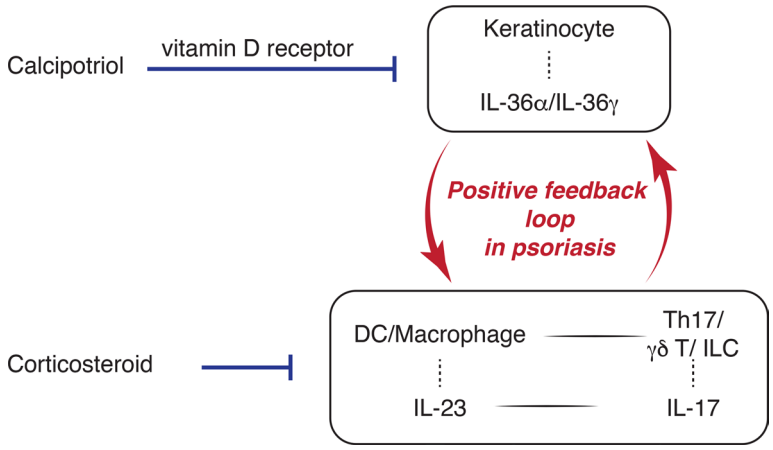

Figure 8. A schematic representation showing that the positive feedback loop of IL-36 and IL-23/IL-17 in psoriasis can be efficiently disrupted by calcipotriol and corticosteroid combination therapy for plaque psoriasis. Calcipotriol acts on keratinocytes to repress the expression of IL-36α/γ, an effect mediated through keratinocytic vitamin D receptor (VDR); on the other hand, corticosteroid acts on immune cells to suppress the IL-23/IL-17 axis (IL-23 produced by DC/macrophages and IL-17 produced by Th17 cells/γδ T cells/innate lymphoid cells [ILC]). By this means, the calcipotriol and corticosteroid combination disrupts efficiently the inflammatory loop, thus achieving a superior efficiency than either agent alone.

Moreover, other atypical nVDREs may exist and function (54, 55). Therefore, ChIP-seq analyses coupled with mutagenesis analyses will be necessary to fully identify the functional nVDREs in the promoters of IL-36α and IL-36γ, as well as to study in depth the regulatory mechanisms.

In contrast with Cal, the decrease of IL-36α/γ expression in mouse psoriasis upon the topical Dex treatment is not mediated by a direct repression. Recently, an interregulation of Th17 cytokines and the IL-36 cytokines has been proposed in psoriasis pathogenesis, which leads to full-blown clinical manifestation (9, 42, 58). Indeed, we showed that, upon Ald treatment, IL-36α/γ expression was induced in the immunodeficient NSG mice (in the absence of IL-17 and IL-22); however, the induction of IL-36α/γ expression was apparently higher in Ald-treated WT mice (Figure 5D). This suggests that IL-36α/γ expression in KCs is positively feedback regulated by cytokines (e.g., IL-17/IL-22) derived from immune cells. It is conceivable that an efficient disruption of the IL-36 and IL-23/IL-17 positive loop can be achieved through the interruption at the 2 critical nodes (i.e., IL-36 in KCs by Cal and IL-23/IL-17 in immune cells by corticosteroid), which thus explain the efficacy of the combined Cal/Dex treatment for psoriasis. It will be interesting to further explore to what extend the disruption of the IL-36/IL-23/IL-17 loop controls various inflammatory mediators identified in psoriasis pathologies, such as TNF-α and IL-6, both of which were observed to be synergistically reduced in Ald-induced psoriatic mice upon Cal/ Dex treatment (Supplemental Figure 6).

In conclusion, our present study has provided potentially novel insights into mechanisms underlying the therapeutic effects of Cal in the treatment of PP, and particularly, it has shown a mechanism underlying the superior therapeutic efficacy achieved by Cal with corticosteroid therapy, which has been recently proved in clinic (20, 21). Based on our findings, it is conceivable that interrupting the inflammatory loop at the IL-36 (KCs) and IL-23/IL-17 (immune cells) dual points should achieve a better effect than monotherapy for psoriasis. In this aspect, it will be highly interesting to test the combination of IL-36–targeting molecules (e.g., Cal) or biologicals (e.g., neutralizing antibodies against IL-36/IL-36R, which are currently under the development) with those therapeutics agents recently developed to target IL-23 or IL-17 pathways (59, 60). It is expected that such a combination will not only improve the efficiency and prevent the recurrences, but also permit the decreased dose of each treatment to reduce side effects, thereby offering potentially new therapeutic strategies for human psoriasis.

Methods

Mice. Mice were bred in IGBMC under specific pathogen-free conditions. Balb/c mice were from Charles River Laboratories, and NSG were from the Jackson Laboratory. *Tslp*$^{-/-}$ (28), *Vdr*$^{-/-}$, and *Vdr*$^{KC-/-}$ (K14-Cre$^{Tg/0}$/ *Vdr*$^{L2/L2}$) (29) mice were all generated by us as described and backcrossed to Balb/c genetic background. Female mice at the age of 8–12 weeks were used in the study.

Mouse treatment. Ald (3M Pharamaceuticals; MEDA AB Pharma) is a commercially available cream that contains 5% IMQ. Mice received, on a daily basis (in the afternoon) and for 4 consecutive days, a dose of 30 mg Ald cream/ear (corresponding to 0.15 mg IMQ/ear). Cal (2 nmol; MilliporeSigma), 10 nmol of Dex (MilliporeSigma), or the combined solution, in 25 μl ETOH were topically applied (in the morning) as indicated in experimental scheme (Figure 1A and Figure 7A).

Ex vivo culture of mouse ear epidermis. Ears from adult mice were disinfected with 10% povidone-iodine solution and were then washed in distilled water and 70% ETOH. Ears were then separated with forceps and floated in a 4 mg/ml of Dispase (Thermo Fisher Scientific) in PBS in a sterile petri dish, with the dermis side down, and incubated overnight at 4°C. After the dermis was removed, epidermis was washed in PBS and then cultured by floating in a medium without carbonate prepared as described (61): DMEM (Invitrogen) was mixed with DMEM/F-12 1:1 (v/v) mixture (Invitrogen) and then adjusted to pH 7.2. The medium was supplemented with 10% FBS (DUTSCHER), cholera toxin (0.1 nM) (MilliporeSigma), mouse epidermal growth factor (10 ng/ml) (MilliporeSigma), 3,3',5'-triiodo-t-thyronine (2 nM) (MilliporeSigma), human apo-transferrin (5 μg/ml) (MilliporeSigma), human insulin (5 μg/ml) (MilliporeSigma), hydrocortisone (0.4 μg/ml) (MilliporeSigma), penicillin (60 μg/ml) (Invitrogen), and gentamicin (25 μg/ml) (KALYS). Cal (1 μM) or 10 μM Dex was added to the culture medium. After 24 hours of ex vivo culture, the epidermis was harvested for RNA extraction and qPCR analyses.

Human primary KC (HPKC) preparation and culture. HPKC were obtained from surgical samples of healthy breast skin. Skin samples were incubated overnight at 4°C in a trypsin solution (trypsin 0.25%, EDTA 0.1%). Epidermal sheets were then removed from the dermis, and cells were dissociated. HPKC were cultured in KC serum-free medium (SFM) supplemented with bovine pituitary extract (25 μg/ml) and recombinant epidermal growth factor (0.25 ng/ml; all from Invitrogen). HPKC were starved for 24 hours in KC SFM without the addition of growth factors before stimulation for 24 hours in the presence or absence of 20 ng/ml of TNF-α, IFN-γ, and/or IL-17 (all from R&D systems).

Human psoriasis patient study. Skin biopsy samples from patients with moderate to severe PP were obtained from the department of dermatology of Bordeaux Hospital. Patients included in this study did not receive topical or systemic treatments for the final 6 weeks. Patients were never treated with biologics. Patient no. 1 (35 years old; Psoriasis Area and Severity Index [PASI] 32.6; patient no. 2 (44 years old; PASI 6.6); patient no. 3 (21 years old; PASI 20.9); patient no. 4 (55 years old; PASI 37). One skin biopsy was performed on lesional skin before and following 4 days of topical treatment with Cal ointment once a day. Both biopsies were performed on the same psoriatic lesion.

Histopathology and IHC staining. Mouse ears were fixed for 24 hours at 4°C in 4% paraformaldehyde and embedded in paraffin. Sections (5 μm) were stained with H&E or IHC staining.

For IHC staining of IL-36α, paraffin sections were treated with 0.6% H_2O_2 (in PBS) to block the endogenous peroxidase activity before antigen retrieving with citric buffer (10 mmol/l citric acid, pH 6). Slides were then blocked with 5% normal rabbit serum (Vector Laboratories) and incubated with goat polyclonal anti–mouse IL-36α antibody (R&D Systems, AF2297, dilution 1:100). Slides were then washed and incubated with HRP-rabbit anti–goat IgG (DAKO, P0449, dilution 1:100). Staining was then visualized with AEC+ high sensitivity substrate chromogen solution (Dako).

For IHC staining of IL-23p19, paraffin sections were treated with 0.6% H_2O_2 (in PBS) to block the endogenous peroxidase activity before antigen retrieving with citric buffer (10 mmol/l citric acid, pH 6). Slides were then blocked with 5% normal goat serum (Vector Laboratories) and incubated with rabbit polyclonal IL-23p19 (Abcam, ab45420, dilution 1:100). Slides were then washed and incubated with biotinylated goat anti–rabbit IgG and treatment of AB complex (Vector Laboratories). Staining was finally visualized with AEC+ high sensitivity substrate chromogen solution (Dako).

For immunofluorescence staining of NIMP-R14, 10-μm cryosections were fixed in 4% paraformaldehyde, permeabilized with acetone, and blocked with 5% normal goat serum (Vector Laboratories). Slides were then incubated with primary antibody (rat monoclonal anti–NIMP-R14 [anti-neutrophil antibody; Abcam, ab2557, dilution 1:750]). After washing, sections were incubated with CY3-conjugated goat anti–rat IgG antibody (Jackson ImmunoResearch, 112-165-167, dilution 1:400) and mounted with Vectashield medium (Vector Laboratories) containing 4'-6-diamidino-2-phenylindole dinhydrochloride (for nuclear staining; Invitrogen).

RNAscope in situ hybridization. Mouse ears were fixed in 10% of neutral buffered formalin and embedded in paraffin. Freshly prepared 5 μm sections were used for RNA in situ hybridization, following the manufacture protocol for RNAscope Red detection Kit (Advanced Cell Diagnostics). To confirm mRNA

integrity in the paraffin sections, Mm-Ppib probe (Mus musculus peptidylprolyl isomerase B) was used as a positive control (62). Mm-dapB probe (Bacterial Bacillus subtilis dihydrodipicolinate reductase) was used as negative control. RNAscope probes used for detection of IL-36α and IL-36γ were MmIL-36α (catalog 403651) and MmIL-36γ (catalog 425241).

RNA extraction and qPCR. Total RNA was extracted from mouse ears or human skin biopsies with Trizol reagent (Invitrogen) according to standard protocol. Total RNA from human primary KC cultures was extracted using Nucleospin RNA kit (Macherey-Nagel), according to manufacturer's instructions. Reverse transcription was performed using random oligonucleotide hexamers and amplified by qPCR with a Lightcycler 480 (Roche Diagnostics) and the QuantiTect SYBR Green kit (Qiagen), according to the manufacturer's instructions. Relative RNA levels were calculated using hypoxanthine phosphoribosyltransferase (HPRT) as internal control. The sequences of primers are listed in the Supplemental Table 1. For the analyses of each set of gene expression, an arbitrary unit of 100 was given to the samples with the highest level, and the remaining samples were plotted relative to this value.

Statistics. Data were analyzed using Sigmaplot (Systat Software Inc.) or GraphPad Prism by 2-tailed Student's *t* test or by the Mann-Whitney rank sum test, depending on results from the Kolmogorov-Smirnov test (with Lilliefors correction) for normality and the Levene Median test for equal variance. Data are presented as means ± SEM. $*P < 0.05$, $**P < 0.01$, $***P < 0.001$ was considered to be statistically significant.

Study approval. All mouse experiments were performed in accordance with the animal care and ethic committee of IGBMC and Institut Clinique de la Souris (ICS). All studies involving human tissues were approved by the local institutional ethics committee (Hôpital Saint-André Service de Dermatologie). All patients gave their written informed consent.

Author contributions

BG, RW, and ML designed research studies; BG, RW, and PH performed experiments; CM, JS, and KB designed and performed studies on human psoriasis patients and human primary KC cultures; TY performed bioinformatic analyses; CG and JY designed and constructed plasmids for studying promoter activity; BG, RW, and ML analyzed and interpreted data, as well as wrote the manuscript. ML directed the study and supervised the work.

Acknowledgments

We thank the staff of animal facilities, genetic engineering, mouse supporting services, flow cytometry, histopathology, microscopy and imaging, and cell culture of IGBMC and Institut Clinique de la Souris (ICS) for excellent technical assistance. We are grateful for the help from P. Kirstett and S. Chan (IGBMC) with NSG mice. We thank P. Chambon (IGBMC) and S. Chan (IGBMC) for a critical reading of the manuscript. We would like to acknowledge the funding supports from l'Agence Nationale de la Recherche (ANR-13-BSV1-0024-01; ANR-15-CE14-0009-03; ANR-17-CE14-0025-01) to ML, from Fondation Recherche Medicale (Equipe FRM 2018) to ML, and the first joint programme of the Freiburg Institute for Advanced Studies (FRIAS) and the University of Strasbourg Institute for Advanced Study (USIAS) to ML and JY. The study was also supported by the grant ANR-10-LABX-0030-INRT, a French State fund managed by the Agence Nationale de la Recherche under the frame program Investissements d'Avenir ANR-10-IDEX-0002-02; the Centre National de la Recherche Scientifique (CNRS); the Institut National de la Santé et de la Recherche Médicale (INSERM), and the Université de Strasbourg (Unistra). BG is an IGBMC International PhD Programme fellow supported by LabEx INRT funds. RW was supported by a PhD fellowship from the Association pour la Recherche à l'IGBMC (ARI).

Address correspondence to: Mei Li, Institut de Génétique et de Biologie Moléculaire et Cellulaire, Illkirch Cedex 67404, France. Phone: 33.3.88.65.35.71; Email: mei@igbmc.fr.

1. Boehncke WH, Schön MP. Psoriasis. *Lancet*. 2015;386(9997):983–994.
2. Parisi R, Symmons DP, Griffiths CE, Ashcroft DM, Identification Management of Psoriasis Associated ComorbidiTy (IMPACT) project team. Global epidemiology of psoriasis: a systematic review of incidence and prevalence. *J Invest Dermatol*. 2013;133(2):377–385.
3. Takeshita J, et al. Psoriasis and comorbid diseases: Epidemiology. *J Am Acad Dermatol*. 2017;76(3):377–390.
4. Di Cesare A, Di Meglio P, Nestle FO. The IL-23/Th17 axis in the immunopathogenesis of psoriasis. *J Invest Dermatol*.

2009;129(6):1339–1350.
5. Lowes MA, Suárez-Fariñas M, Krueger JG. Immunology of psoriasis. *Annu Rev Immunol*. 2014;32:227–255.
6. Boutet MA, et al. Distinct expression of interleukin (IL)-36α, β and γ, their antagonist IL-36Ra and IL-38 in psoriasis, rheumatoid arthritis and Crohn's disease. *Clin Exp Immunol*. 2016;184(2):159–173.
7. Blumberg H, et al. Opposing activities of two novel members of the IL-1 ligand family regulate skin inflammation. *J Exp Med*. 2007;204(11):2603–2614.
8. Johnston A, et al. IL-1F5, -F6, -F8, and -F9: a novel IL-1 family signaling system that is active in psoriasis and promotes keratinocyte antimicrobial peptide expression. *J Immunol*. 2011;186(4):2613–2622.
9. Carrier Y, et al. Inter-regulation of Th17 cytokines and the IL-36 cytokines in vitro and in vivo: implications in psoriasis pathogenesis. *J Invest Dermatol*. 2011;131(12):2428–2437.
10. Keermann M, Kõks S, Reimann E, Prans E, Abram K, Kingo K. Transcriptional landscape of psoriasis identifies the involvement of IL36 and IL36RN. *BMC Genomics*. 2015;16:322.
11. Mahil SK, et al. An analysis of IL-36 signature genes and individuals with IL1RL2 knockout mutations validates IL-36 as a psoriasis therapeutic target. *Sci Transl Med*. 2017;9(411):eaan2514.
12. D'Erme AM, et al. IL-36γ (IL-1F9) is a biomarker for psoriasis skin lesions. *J Invest Dermatol*. 2015;135(4):1025–1032.
13. Ganesan R, et al. Generation and functional characterization of anti-human and anti-mouse IL-36R antagonist monoclonal antibodies. *MAbs*. 2017;9(7):1143–1154.
14. Milora KA, Fu H, Dubaz O, Jensen LE. Unprocessed Interleukin-36α Regulates Psoriasis-Like Skin Inflammation in Cooperation With Interleukin-1. *J Invest Dermatol*. 2015;135(12):2992–3000.
15. Tortola L, et al. Psoriasiform dermatitis is driven by IL-36-mediated DC-keratinocyte crosstalk. *J Clin Invest*. 2012;122(11):3965–3976.
16. Bridgewood C, et al. IL-36γ Is a Strong Inducer of IL-23 in Psoriatic Cells and Activates Angiogenesis. *Front Immunol*. 2018;9:200.
17. Chi HH, et al. IL-36 Signaling Facilitates Activation of the NLRP3 Inflammasome and IL-23/IL-17 Axis in Renal Inflammation and Fibrosis. *J Am Soc Nephrol*. 2017;28(7):2022–2037.
18. Menter A, Griffiths CE. Current and future management of psoriasis. *Lancet*. 2007;370(9583):272–284.
19. Trémezaygues L, Reichrath J. Vitamin D analogs in the treatment of psoriasis: Where are we standing and where will we be going? *Dermatoendocrinol*. 2011;3(3):180–186.
20. Rogalski C. Calcipotriol/betamethasone for the treatment of psoriasis: efficacy, safety, and patient acceptability. *Psoriasis (Auckl)*. 2015;5:97–107.
21. Patel NU, Felix K, Reimer D, Feldman SR. Calcipotriene/betamethasone dipropionate for the treatment of psoriasis vulgaris: an evidence-based review. *Clin Cosmet Investig Dermatol*. 2017;10:385–391.
22. van der Fits L, et al. Imiquimod-induced psoriasis-like skin inflammation in mice is mediated via the IL-23/IL-17 axis. *J Immunol*. 2009;182(9):5836–5845.
23. Flutter B, Nestle FO. TLRs to cytokines: mechanistic insights from the imiquimod mouse model of psoriasis. *Eur J Immunol*. 2013;43(12):3138–3146.
24. Hawkes JE, Gudjonsson JE, Ward NL. The Snowballing Literature on Imiquimod-Induced Skin Inflammation in Mice: A Critical Appraisal. *J Invest Dermatol*. 2017;137(3):546–549.
25. Gilliet M, et al. Psoriasis triggered by toll-like receptor 7 agonist imiquimod in the presence of dermal plasmacytoid dendritic cell precursors. *Arch Dermatol*. 2004;140(12):1490–1495.
26. Lovato P, Norsgaard H, Tokura Y, Røpke MA. Calcipotriol and betamethasone dipropionate exert additive inhibitory effects on the cytokine expression of inflammatory dendritic cell-Th17 cell axis in psoriasis. *J Dermatol Sci*. 2016;81(3):153–164.
27. Kusuba N, et al. Inhibition of IL-17-committed T cells in a murine psoriasis model by a vitamin D analogue. *J Allergy Clin Immunol*. 2018;141(3):972–981.e10.
28. Li M, Hener P, Zhang Z, Ganti KP, Metzger D, Chambon P. Induction of thymic stromal lymphopoietin expression in keratinocytes is necessary for generating an atopic dermatitis upon application of the active vitamin D3 analogue MC903 on mouse skin. *J Invest Dermatol*. 2009;129(2):498–502.
29. Li M, Hener P, Zhang Z, Kato S, Metzger D, Chambon P. Topical vitamin D3 and low-calcemic analogs induce thymic stromal lymphopoietin in mouse keratinocytes and trigger an atopic dermatitis. *Proc Natl Acad Sci USA*. 2006;103(31):11736–11741.
30. Cai Y, et al. Pivotal role of dermal IL-17-producing γδ T cells in skin inflammation. *Immunity*. 2011;35(4):596–610.
31. Wohn C, et al. Langerin(neg) conventional dendritic cells produce IL-23 to drive psoriatic plaque formation in mice. *Proc Natl Acad Sci USA*. 2013;110(26):10723–10728.
32. Trochoutsou AI, Kloukina V, Samitas K, Xanthou G. Vitamin-D in the Immune System: Genomic and Non-Genomic Actions. *Mini Rev Med Chem*. 2015;15(11):953–963.
33. Köllisch G, et al. Various members of the Toll-like receptor family contribute to the innate immune response of human epidermal keratinocytes. *Immunology*. 2005;114(4):531–541.
34. Lebre MC, et al. Human keratinocytes express functional Toll-like receptor 3, 4, 5, and 9. *J Invest Dermatol*. 2007;127(2):331–341.
35. Leyva-Castillo JM, et al. Skin thymic stromal lymphopoietin initiates Th2 responses through an orchestrated immune cascade. *Nat Commun*. 2013;4:2847.
36. Li M, Messaddeq N, Teletin M, Pasquali JL, Metzger D, Chambon P. Retinoid X receptor ablation in adult mouse keratinocytes generates an atopic dermatitis triggered by thymic stromal lymphopoietin. *Proc Natl Acad Sci USA*. 2005;102(41):14795–14800.
37. Li J, et al. Counterregulation between thymic stromal lymphopoietin- and IL-23-driven immune axes shapes skin inflammation in mice with epidermal barrier defects. *J Allergy Clin Immunol*. 2016;138(1):150–161.e13.
38. Onoufriadis A, et al. Mutations in IL36RN/IL1F5 are associated with the severe episodic inflammatory skin disease known as generalized pustular psoriasis. *Am J Hum Genet*. 2011;89(3):432–437.
39. Tauber M, et al. IL36RN Mutations Affect Protein Expression and Function: A Basis for Genotype-Phenotype Correlation in Pustular Diseases. *J Invest Dermatol*. 2016;136(9):1811–1819.
40. Swindell WR, et al. Imiquimod has strain-dependent effects in mice and does not uniquely model human psoriasis. *Genome Med*. 2017;9(1):24.

41. Palma L, Sfara C, Antonelli A, Magnani M. Dexamethasone restrains ongoing expression of interleukin-23p19 in peripheral blood-derived human macrophages. *BMC Pharmacol*. 2011;11:8.
42. Pfaff CM, Marquardt Y, Fietkau K, Baron JM, Lüscher B. The psoriasis-associated IL-17A induces and cooperates with IL-36 cytokines to control keratinocyte differentiation and function. *Sci Rep*. 2017;7(1):15631.
43. Seehus CR, et al. The development of innate lymphoid cells requires TOX-dependent generation of a common innate lymphoid cell progenitor. *Nat Immunol*. 2015;16(6):599–608.
44. Morizane S, Nomura H, Tachibana K, Nakagawa Y, Iwatsuki K. The synergistic activities of the combination of tumour necrosis factor-α, interleukin-17A and interferon-γ in epidermal keratinocytes. *Br J Dermatol*. 2018;179(2):496–498.
45. Glitzner E, et al. Specific roles for dendritic cell subsets during initiation and progression of psoriasis. *EMBO Mol Med*. 2014;6(10):1312–1327.
46. Terhorst D, et al. Dynamics and Transcriptomics of Skin Dendritic Cells and Macrophages in an Imiquimod-Induced, Biphasic Mouse Model of Psoriasis. *J Immunol*. 2015;195(10):4953–4961.
47. Singh TP, et al. Monocyte-derived inflammatory Langerhans cells and dermal dendritic cells mediate psoriasis-like inflammation. *Nat Commun*. 2016;7:13581.
48. Liu H, et al. Staphylococcus aureus Epicutaneous Exposure Drives Skin Inflammation via IL-36-Mediated T Cell Responses. *Cell Host Microbe*. 2017;22(5):653–666.e5.
49. Suárez-Fariñas M, et al. RNA sequencing atopic dermatitis transcriptome profiling provides insights into novel disease mechanisms with potential therapeutic implications. *J Allergy Clin Immunol*. 2015;135(5):1218–1227.
50. Swindell WR, et al. RNA-Seq Analysis of IL-1B and IL-36 Responses in Epidermal Keratinocytes Identifies a Shared MyD88-Dependent Gene Signature. *Front Immunol*. 2018;9:80.
51. Kurinna S, et al. Autocrine and Paracrine Regulation of Keratinocyte Proliferation through a Novel Nrf2-IL-36γ Pathway. *J Immunol*. 2016;196(11):4663–4670.
52. Zhou L, et al. Quantitative ligand and receptor binding studies reveal the mechanism of interleukin-36 (IL-36) pathway activation. *J Biol Chem*. 2018;293(2):403–411.
53. Jiang Z, et al. IL-36γ Induced by the TLR3-SLUG-VDR Axis Promotes Wound Healing via REG3A. *J Invest Dermatol*. 2017;137(12):2620–2629.
54. Swami S, Krishnan AV, Peng L, Lundqvist J, Feldman D. Transrepression of the estrogen receptor promoter by calcitriol in human breast cancer cells via two negative vitamin D response elements. *Endocr Relat Cancer*. 2013;20(4):565–577.
55. Turunen MM, Dunlop TW, Carlberg C, Väisänen S. Selective use of multiple vitamin D response elements underlies the 1 alpha,25-dihydroxyvitamin D3-mediated negative regulation of the human CYP27B1 gene. *Nucleic Acids Res*. 2007;35(8):2734–2747.
56. Grant CE, Bailey TL, Noble WS. FIMO: scanning for occurrences of a given motif. *Bioinformatics*. 2011;27(7):1017–1018.
57. Mathelier A, et al. JASPAR 2016: a major expansion and update of the open-access database of transcription factor binding profiles. *Nucleic Acids Res*. 2016;44(D1):D110–D115.
58. Furue K, et al. Highlighting Interleukin-36 Signalling in Plaque Psoriasis and Pustular Psoriasis. *Acta Derm Venereol*. 2018;98(1):5–13.
59. Conrad C, Gilliet M. Psoriasis: from Pathogenesis to Targeted Therapies. *Clin Rev Allergy Immunol*. 2018;54(1):102–113.
60. Mahil SK, Capon F, Barker JN. Update on psoriasis immunopathogenesis and targeted immunotherapy. *Semin Immunopathol*. 2016;38(1):11–27.
61. Mazzalupo S, Wawersik MJ, Coulombe PA. An ex vivo assay to assess the potential of skin keratinocytes for wound epithelialization. *J Invest Dermatol*. 2002;118(5):866–870.
62. Bingham V, et al. RNAscope in situ hybridization confirms mRNA integrity in formalin-fixed, paraffin-embedded cancer tissue samples. *Oncotarget*. 2017;8(55):93392–93403.